

## Sympathetic nucleation of austenite in a Fe–22Cr–5Ni duplex stainless steel

C.Y. Chen, H.W. Yen and J.R. Yang\*

*Department of Materials Science and Engineering, National Taiwan University, Taipei 106, Taiwan*

Received 12 October 2006; revised 24 December 2006; accepted 24 December 2006

Available online 26 January 2007

In a Fe–22Cr–5Ni duplex stainless steel,  $\delta$ -ferrite in a very high supersaturated solid solution state was found to promote the formation of the intragranularly nucleated austenite. Transmission electron microscopy revealed that, after the initial nucleation events for intragranularly nucleated austenite, the subsequent small particle of austenite could form sympathetically at the broad face of the prior austenite grain. The orientation relationship between adjacent grains of sympathetically nucleated austenite has been investigated.

© 2007 Acta Materialia Inc. Published by Elsevier Ltd. All rights reserved.

*Keywords:* Stainless steel; Isothermal heat treatments; TEM; Electron diffraction; Sympathetic nucleation

Duplex stainless steels (DSS) have been used for a variety of applications in marine construction, the chemical industry and power plants [1,2] due to their combining the attractive properties of fully austenitic and fully ferritic stainless steels. Despite DSS being prevalent in the last two decades, it is still deemed necessarily to improve their properties further, i.e. higher strength, greater toughness, etc. In this respect, refining the microstructure of DSS would be a significant advantage. Some related methods [3,4] for microstructural refinement have been proved to be effective. The current work is based on a simple heat treatment to study the isothermal transformation of  $\delta$ -ferrite to austenite in the two-phase region through a supersaturated solid solution of  $\delta$ -ferrite matrix. This method is much interesting because the refined austenite in the duplex microstructure could be produced solely by utilizing solid-state phase transformation without resorting to alloying or thermomechanical treatment.

A commercial Fe–22 wt.% Cr–5 wt.% Ni (so-called 2205) duplex stainless steel was studied to determine the effect of the degree of supersaturation in  $\delta$ -ferrite matrix on the subsequent isothermal transformation of  $\delta$ -ferrite to austenite at 1150 °C. The morphology and crystallography characteristic of austenite precipitate

were examined using optical metallography and transmission electron microscopy (TEM), respectively. For the purpose of revealing the orientation relationship between adjacent grains of austenite, axis/angle pairs were derived from the corresponding selected-area electron diffraction patterns. It was expected that intragranular nucleation of austenite would occur, since the grain size of prior  $\delta$ -ferrite matrix was extremely large.

The experimental material was a commercial 2205 duplex stainless steel bar (53 mm diameter) produced by Gloria Material Technology Corporation through the fourfold forging of a cast slab at 1160–1180 °C and annealing at 1050 °C for 30 min, followed by water quenching to give a dual-phase structure without other second phases. The chemical composition of the alloy was Fe–0.02C–0.38Si–1.47Mn–22.62Cr–5.12Ni–3.24Mo (wt.%) with trace elements 0.196N–0.022P–0.001S (wt.%). Dilatometer specimens 6 mm in length and 3 mm in diameter were machined from the half radius positions of the original bar along the longitudinal direction. All the heat treatment processes were carried out on a Dilatometric III RDP dilatometer from Theta Industries, Inc. The dilatometer was interfaced with a computer workstation (PDP 11/55 central processor) for analyzing the resulting data. A software package (provided by Theta Industries) was used to flexibly control the execution of the isothermal transformation experiments. A vacuum of  $10^{-5}$  torr was maintained to protect specimens from oxidation during the process.

\* Corresponding author. Tel.: +886 2 23632756; fax: +886 2 23634562; e-mail: [jryang@ntu.edu.tw](mailto:jryang@ntu.edu.tw)

This work was focused on the isothermal transformation of  $\delta$ -ferrite to austenite through a supersaturated state of  $\delta$ -ferrite matrix. After solution treatment at 1350 °C for 3 min, the specimens were rapidly cooled to ambient temperature at a cooling rate of 100 °C s<sup>-1</sup>. As a result, a supersaturated solid solution of  $\delta$ -ferrite matrix (with the grain size about 450  $\mu$ m) was obtained. The specimens were immediately heated up to 1150 °C, held at this temperature for various time intervals from 30 s to 20 min, and then rapidly cooled to room temperature at the rate of 100 °C s<sup>-1</sup>.

The samples for optical metallography, prepared from dilatometer specimens, were mechanically polished and then electrically etched in 10 N NaOH solution at 9 V etching potential. In the optical metallographs,  $\delta$ -ferrite and austenite were distinguished by the contrast of gray and white, respectively. Thin foils for TEM were prepared from 0.25 mm thick disks sliced from dilatometer specimens. The disks were thinned to 0.07 mm by abrasion on SiC papers and twin-jet electropolished using a mixture of 5% perchloric acid, 25% glycerol and 70% ethanol at ambient temperature and with a 45 V etching potential. They were examined using a JEOL JEM-2000EX transmission electron microscope operated at 200 kV.

Figure 1a–d presents a series of optical metallographs obtained from the specimens isothermally treated at 1150 °C for four different holding times (from 30 s to 20 min). They show that the white etched austenite islands are dispersed in the gray etched  $\delta$ -ferrite matrix, and that the volume fraction of austenite increases with increasing isothermal heat treating time. On the basis of Thermo-Calc., the variation of the phase amounts as a function of temperature for the steel studied has been calculated; it indicates that the structure tends to be completely ferritized at 1350 °C and that the volume fraction of austenite in the equilibrium state at 1150 °C is about 0.4. The measured volume fraction of  $\gamma$ -phase in the specimen isothermally treated at 1150 °C for 20 min is also near 0.4; the corresponding optical micrograph is shown in Figure 1d. Very fine

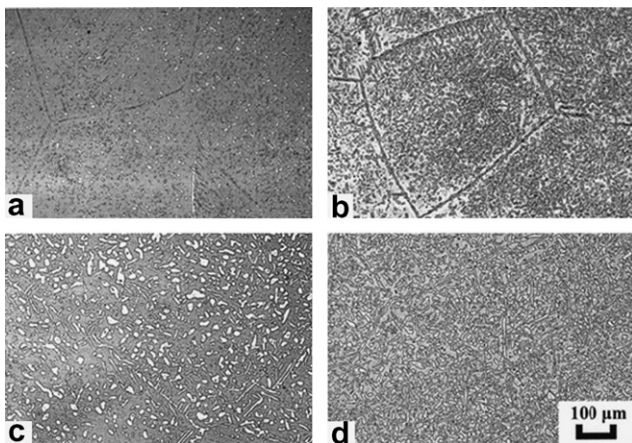


**Figure 1.** Optical metallographs showing the development of microstructure for specimens isothermally treated at 1150 °C for the variety of isothermal holding times: (a) 30 s, (b) 5 min, (c) 10 min and (d) 20 min.

austenite particles, which were intragranularly nucleated within  $\delta$ -ferrite matrix, were obtained. The detailed morphology of intragranularly nucleated austenite has been studied and will be presented later. The state of  $\delta$ -ferrite prior transformation is of primary importance as it influences the nucleation sites for the formation of austenite. It is clear that, after solution treatment at 1350 °C for 3 min, rapid cooling (at a cooling rate of 100 °C s<sup>-1</sup>) to ambient temperature leads to an extremely coarse-grained  $\delta$ -ferrite matrix in a very high supersaturated solid solution state. Furthermore, the high quenching rate could induce large quantities of vacancies and defects (e.g. intrinsic stacking faults) in the matrix. These complex factors would promote nucleation of austenite at the intragranular heterogeneities. The striking feature shown in Figure 1 distinctly confirms the structural refinement for the present heat treatment.

Using optical microscopy, it is apparent that these products of the coarse-grained  $\delta$ -ferrite decomposition in the 2205 duplex stainless steel have an intragranularly nucleated morphology that is roughly similar to those of the coarse-grained  $\gamma$  decomposition in a typical alloy steel weld metal [5,6]. In the latter case, acicular ferrite has been well known to be intragranularly nucleated with bainitic ferrite, which is associated with a displacive transformation [6,7]. During the initial stages of transformation, the nucleation of acicular ferrite occurs heterogeneously at non-metallic inclusions present in the coarse-grained austenite matrix of steel weld deposits. The sympathetic nucleation of acicular ferrite has been recognized as follows. After the initial nucleation events at inclusions, the newly formed acicular ferrite grains can nucleate on the existing acicular ferrite/austenite interfaces. The growth of acicular ferrite is accompanied by an invariant-plane strain deformation. Therefore, the subsequent autocatalytic nucleation of acicular ferrite could be triggered by the strain state in the vicinity of the prior acicular ferrite plate. On the other hand, in this work the growth of austenite at a high temperature is involved with a diffusional transformation, and the intragranularly nucleated austenite can also be seen to grow in clusters (as shown in Fig. 2), which indicate that the austenite particles nucleate sympathetically. No research work on sympathetic nucleation of austenite has yet been reported. The purpose of the present work is to explore this aspect.

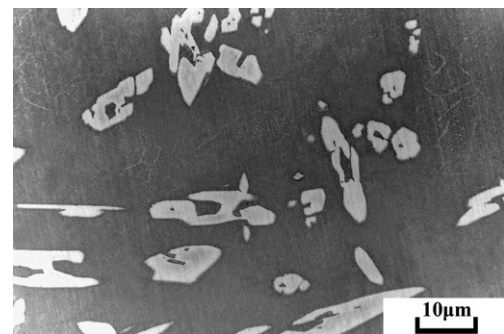


**Figure 2.** Optical metallograph (taken from specimens isothermally treated at 1150 °C for 30 s) showing that intragranularly nucleated austenite grains grow in clusters.

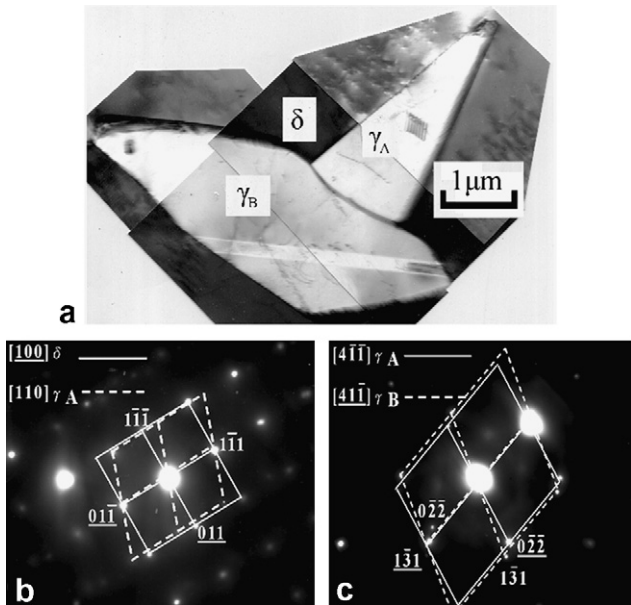


**Figure 3.** TEM showing: (a) the sympathetic nucleation feature of intragranularly nucleated austenite; (b) and (c) selected-area diffraction patterns obtained from  $\delta/\gamma_A$  and  $\gamma_A/\gamma_B$ , respectively.

The typical morphology of sympathetically nucleated austenite has been investigated by TEM, as illustrated in Figure 3; it is apparent that, after the initial nucleation event for intragranularly nucleated austenite, the subsequent small particle of austenite forms at the broad face of the prior large austenite grain. In order to reveal the orientation relationship between neighboring grains of austenite, the corresponding selected-area electron diffraction patterns were examined. It should be noted that the grains of intragranularly nucleated austenite can appear to be adjacent to one another for two reasons: sympathetic nucleation (the formation of one grain may stimulate the growth of another) and hard impingement (grains which have nucleated at completely separate sites may come into contact as a consequence of impingement). It is difficult to distinguish between sympathetic nucleation and hard impingement in the specimens isothermally treated for a longer time because hard impingement will be a sufficiently likely result of the different nucleation-site austenite particles growing in contact with each other. Therefore, in this work care was taken to examine only the case of sympathetic nucleation from the specimens isothermally treated at 1150 °C for 30 s; under TEM observation at low magnification, sympathetically nucleated grains can be identified in a form of cluster, where the small austenite particle forms at the broad face of the prior large austenite grain (see another example in Ref. [8]). The electron diffraction patterns for sympathetically nucleated austenite grains in Figure 3c shows that the adjacent grains have a very similar orientation in space. The orientation relationship between a pair of like crystals, the crystallographic bases of which are defined from a common origin, can be presented using a rotation matrix. From the rotation matrix, a corresponding axis/angle pair can be derived. This infers that, if one of the crystals is rigidly rotated about the specified axis which passes

through the original, through a right-handed angle of rotation  $\theta$ , its orientation coincides with that of the other. For each pair of austenite (face-centered cubic, fcc) crystals, there are 24 crystallographically equivalent descriptions [9] in terms of axis angle pairs or rotation matrices. In the present work, the equivalent axis angle pair with the greatest angle of rotation was chosen for each pair of adjacent austenite grains in order to interpret the data clearly. The results for four pairs of sympathetically nucleated austenite grains,  $\gamma_A/\gamma_B$ ,  $\gamma_B/\gamma_C$ ,  $\gamma_D/\gamma_E$  and  $\gamma_E/\gamma_F$ , are presented in Table 1. It can be seen that the adjacent austenite grains are similarly orientated in space, the axis angle pairs being close to the symmetry operations  $180^\circ$  about  $\langle 001 \rangle$  or  $180^\circ$  about  $\langle 011 \rangle$  of the fcc structure.

The intragranularly nucleated austenite is presumed to exist in a Nishiyama–Wasserman (NW) or Kurdjumov–Sachs (KS) orientation relationship (OR) with  $\delta$ -ferrite matrix; Figure 3b displays the case for the NW OR. The full analyses of all possible results for the NW and KS ORs between  $\delta$  and  $\gamma$ -lattices are presented in Tables 2 and 3, respectively. Six groups can be assigned to six independent  $\{011\}_\delta$  planes in a given  $\delta$  ferrite crystal. Hence, 12 NW and 24 KS independent variants can be obtained. In the cases of both NW and KS, poles of a close-packed plane of  $\delta$   $\{011\}_\delta$  and  $\gamma$   $\{111\}_\gamma$  are parallel to each other, i.e.  $\langle 011 \rangle_\delta \parallel \langle 111 \rangle_\gamma$ . A symmetry operation on the  $\delta$ -lattice of a rotation of  $180^\circ$  about the  $\langle 011 \rangle_\delta$  direction is equivalent to a twinning rotation of  $180^\circ$  about the  $\langle 111 \rangle_\gamma$  direction. Thereby, 12 NW and 24 KS relationships have the special property that variants of austenite can be twin-related in pairs (such as variants 1a–1b, 2a–2b, 3a–3b, ... for NW in Table 2; variants 1a–1b, 1c–1d, 2a–2b, 2c–2d, 3a–3b, 3c–3d, ... for KS in Table 3). By comparing the data of Table 1 with the results in Tables 2 and 3, it seems that the experimental axis angle pairs can be considered approximately as resulting from the existence of NW or KS ORs. However, it is quite plain that in Table 2 only variants 2b, 4b and 5a of NW ORs cause austenite grains to be similarly orientated with respect to variant 1a. Similarly in Table 3, only variants 1c, 3a, 3c, 4a, 6b and 6d of NW ORs cause austenite grains to be similarly orientated with respect to variant 1a. If all possible austenite grains form with equal probability via NW or KS, then only a quarter of austenite grains would have a similar orientation in space. It is therefore suggested that sympathetic nucleation of austenite, which forms by a diffusional transformation at a high temperature, can be easily promoted if adjacent grains of austenite tend to form in a similar orientation.

In summary, the formation of intragranularly nucleated austenite within an extremely coarse-grained  $\delta$ -ferrite matrix, which was in a very high supersaturated

**Table 1.** Orientation relationships described via axis angle pairs

Number	Axis angle pairs	
1	$[-0.1924 \ 0.9623 \ 0.1925]$	$180^\circ$
2	$[0.0823 \ 0.6176 \ 0.7822]$	$180^\circ$
3	$[0.6886 \ 0.0521 \ 0.7233]$	$180^\circ$
4	$[0.6998 \ 0.0213 \ 0.7140]$	$180^\circ$



**Table 2.** Axis angle pairs (with respect to  $\gamma$ ) relating variant **1a** to other variants of austenite that may form within the same  $\delta$ -ferrite crystal with an NW OR

	$\delta$ orientation	Axis angle pair ( $\gamma$ )	Equivalent axis angle pair
1a	(011)[100]	[1.0000 0.0000 0.0000] 0°	–
1b	(011)[–100]	[0.5774 0.5774 0.5774] 180°	$\langle 0.8165 \ 0.4082 \ 0.4082 \rangle 180^\circ$
2a	(101)[010]	[–0.8796 –0.0632 –0.4714] 120°	$\langle 0.8633 \ 0.3998 \ 0.3080 \rangle 175^\circ$
2b	(101)[0–10]	[0.1196 0.1196 0.9856] 90°	$\langle 0.9928 \ 0.1196 \ 0.0072 \rangle 180^\circ$
3a	(110)[001]	[0.8796 0.0632 0.4714] 120°	$\langle 0.8633 \ 0.3998 \ 0.3080 \rangle 180^\circ$
3b	(110)[00–1]	[–0.6969 –0.6969 0.1691] 90°	$\langle 0.6969 \ 0.5845 \ 0.4155 \rangle 180^\circ$
4a	(01–1)[100]	[0.7071 –0.7071 0.0000] 90°	$\langle 0.7071 \ 0.5000 \ 0.5000 \rangle 180^\circ$
4b	(01–1)[–100]	[–0.6969 –0.6969 0.1691] 180°	$\langle 0.9856 \ 0.1196 \ 0.1196 \rangle 180^\circ$
5a	(10–1)[010]	[–0.9928 0.0072 0.1196] 180°	$\langle 0.9928 \ 0.1196 \ 0.0072 \rangle 180^\circ$
5b	(10–1)[0–10]	[0.0749 –0.7416 0.6666] 120°	$\langle 0.8633 \ 0.3998 \ 0.3080 \rangle 175^\circ$
6a	(–110)[001]	[0.6969 0.6969 –0.1691] 90°	$\langle 0.6969 \ 0.5845 \ 0.4155 \rangle 180^\circ$
6b	(–110)[00–1]	[–0.0632 –0.8796 –0.4714] 120°	$\langle 0.8633 \ 0.3998 \ 0.3080 \rangle 175^\circ$

When the  $\delta$ – $\gamma$  orientation is described by the Nishiyama–Wasserman relationship, the  $\{011\}_\delta$  plane should be taken to be parallel to the  $(111)_\gamma$  plane, and the  $\langle 100 \rangle_\delta$  direction should be taken to be parallel to the  $[1-10]_\gamma$  direction.

**Table 3.** Axis angle pairs (with respect to  $\gamma$ ) relating variant **1a** to other variants of austenite that may form within the same  $\delta$ -ferrite crystal with a KS OR

	$\delta$ orientation	Axis angle pair ( $\gamma$ )	Equivalent axis angle pair
1a	(011)[1–11]	[1.000 0.0000 0.0000] 0°	–
1b	(011)[–11–1]	[0.5774 0.5774 0.5774] 180°	$\langle 0.8165 \ 0.4082 \ 0.4082 \rangle 180^\circ$
1c	(011)[–1–11]	[–0.7416 0.0749 0.6667] 180°	$\langle 0.7416 \ 0.6667 \ 0.0749 \rangle 180^\circ$
1d	(011)[11–1]	[–0.3417 0.8130 –0.4714] 180°	$\langle 0.8131 \ 0.4713 \ 0.3418 \rangle 180^\circ$
2a	(101)[11–1]	[–0.8995 –0.4282 –0.0865] 120°	$\langle 0.8624 \ 0.4166 \ 0.2875 \rangle 179^\circ$
2b	(101)[–1–11]	[0.6498 –0.1666 0.7416] 90°	$\langle 0.6965 \ 0.5839 \ 0.4170 \rangle 175^\circ$
2c	(101)[1–1–1]	[–0.1492 –0.6206 0.7698] 120°	$\langle 0.7338 \ 0.5630 \ 0.3802 \rangle 177^\circ$
2d	(101)[–111]	[0.4065 –0.7482 –0.5244] 180°	$\langle 0.7482 \ 0.5244 \ 0.4065 \rangle 180^\circ$
3a	(110)[1–1–1]	[–0.1666 –0.9832 –0.0749] 90°	$\langle 0.9916 \ 0.1207 \ 0.0458 \rangle 179^\circ$
3b	(110)[–111]	[0.8995 0.4282 0.0865] 120°	$\langle 0.8624 \ 0.4166 \ 0.2875 \rangle 179^\circ$
3c	(110)[1–11]	[0.0649 0.0649 –0.9958] 180°	$\langle 0.7041 \ 0.7041 \ 0.0918 \rangle 180^\circ$
3d	(110)[–11–1]	[0.7071 –0.7071 0.0000] 120°	$\langle 0.6124 \ 0.6124 \ 0.5000 \rangle 180^\circ$
4a	(01–1)[–1–1–1]	[–0.1666 –0.9832 –0.0749] 180°	$\langle 0.9832 \ 0.1666 \ 0.0749 \rangle 180^\circ$
4b	(01–1)[111]	[0.7416 –0.0749 –0.6667] 90°	$\langle 0.7046 \ 0.5378 \ 0.4629 \rangle 176^\circ$
4c	(01–1)[1–1–1]	[–0.6498 0.1666 –0.7416] 180°	$\langle 0.7416 \ 0.6498 \ 0.1666 \rangle 180^\circ$
4d	(01–1)[–111]	[0.7416 –0.0749 –0.6667] 90°	$\langle 0.7046 \ 0.5378 \ 0.4629 \rangle 176^\circ$
5a	(–101)[111]	[0.6498 –0.1666 0.7416] 90°	$\langle 0.6965 \ 0.5839 \ 0.4170 \rangle 175^\circ$
5b	(–101)[–1–1–1]	[0.0433 0.5146 0.8563] 120°	$\langle 0.7421 \ 0.5003 \ 0.4460 \rangle 176^\circ$
5c	(–101)[1–11]	[0.6422 0.6422 –0.4184] 180°	$\langle 0.9083 \ 0.2959 \ 0.2959 \rangle 180^\circ$
5d	(–101)[–11–1]	[–0.7071 0.7071 0.0000] 120°	$\langle 0.6124 \ 0.6124 \ 0.5000 \rangle 180^\circ$
6a	(1–10)[–1–1–1]	[–0.1492 –0.6206 0.7698] 120°	$\langle 0.7338 \ 0.5630 \ 0.3802 \rangle 177^\circ$
6b	(1–10)[111]	[–0.9839 0.1708 –0.0530] 180°	$\langle 0.9839 \ 0.1708 \ 0.0530 \rangle 180^\circ$
6c	(1–10)[–1–11]	[0.0433 0.5146 0.8563] 120°	$\langle 0.7421 \ 0.5003 \ 0.4460 \rangle 176^\circ$
6d	(1–10)[11–1]	[–0.1666 –0.9832 –0.0749] 90°	$\langle 0.9916 \ 0.1207 \ 0.0458 \rangle 179^\circ$

When the  $\delta$ – $\gamma$  orientation is described by the Kurdjumov–Sachs relationship, the  $\{011\}_\delta$  plane should be taken to be parallel to the  $(111)_\gamma$  plane, and the  $\langle 1-11 \rangle_\delta$  direction should be taken to be parallel to the  $[1-10]_\gamma$  direction.

solid solution state, has been investigated. The adjacent grains of sympathetically nucleated austenite (via a diffusional transformation) have approximately the same orientation in space.

This work was carried out with the financial support from the National Science Council of the Republic of China, Taiwan, under Contract NSC94-2216-E-011. The authors thank Gloria Material Technology Corporation for the supply of the steel bar.

Supplementary data associated with this article can be found, in the online version, at doi:10.1016/j.scriptamat.2006.12.021.

- [1] J.O. Nilsson, Mater. Sci. Technol. 8 (1992) 685.
- [2] F. Dupouiron, J.P. Audouard, Scand. J. Metall. 25 (1996) 685.
- [3] B. Soyulu, R.W.K. Honeycombe, Mater. Sci. Technol. 7 (1991) 137.
- [4] T. Maki, T. Furuhashi, K. Tsuzaki, ISIJ Int. 41 (2001) 571.
- [5] R.A. Ricks, P.R. Howell, G.S. Barritte, J. Mater. Sci. 17 (1982) 732.
- [6] J.R. Yang, H.K.D.H. Bhadeshia, J. Mater. Sci. 26 (1991) 839.
- [7] H.K.D.H. Bhadeshia, Bainite in Steels, 2nd ed., Institute of Materials, London, 2001.
- [8] T.H. Chen, J.R. Yang, Mater. Sci. Eng. A 338 (2002) 166.
- [9] H.K.D.H. Bhadeshia, Worked Examples in the Geometry of Crystals, 2nd ed., Institute of Materials, London, 2001.